The Holocene

Sub sea surface temperatures in the Polar North Atlantic during the Holocene: Planktic foraminiferal Mg/Ca temperature reconstructions

Journal:	*The Holocene*
Manuscript ID:	HOL-13-0053.R1
Manuscript Type:	Paper
Date Submitted by the Author:	n/a

Complete List of Authors:	Aagaard-Sørensen, Steffen; University of Tromsø, Department of Geology Husum, Katrine; University of Tromsø, Department of Geology Hald, Morten; University of Tromsø, Department of Geology Marchitto, Thomas; University of Colorado, Department of Geological Sciences and Institute of Arctic and Alpine Research Godtliebsen, Fred; University of Tromsø, Department of Mathematics and Statistics

Keywords:	Paleoceanography, Polar North Atlantic, Fram Strait, Atlantic water, Trace elements, sub SST reconstruction

Abstract:	Holocene sea surface temperatures in the eastern Fram Strait are reconstructed based on Mg/Ca ratios measured on the planktic foraminifer *Neogloboquadrina pachyderma* (sin). The reconstructed sub sea surface temperatures ($sSST_{Mg/Ca}$) fluctuate markedly during the earliest Holocene at ~11.7–10.5 ka BP. This probably is in response to the varying presence of sea ice and deglacial melt water. Between ~10.5–7.9 ka BP the $sSST_{Mg/Ca}$ values are relatively high (~4°C) and more stable reflecting high insolation and intensified poleward advection of Atlantic water. After 7.9 ka BP the $sSST_{Mg/Ca}$ decline to an average of ~3°C throughout the mid-Holocene. These changes can be attributed to a combined effect of reduced poleward oceanic heat advection and a decline in insolation as well as a gradually increased influence of eastward migrating Arctic Water. The $sSST_{Mg/Ca}$ increase and vary between 2.1–5.8°C from ~2.7 ka BP to the present. This warming is in contrast to declining late Holocene insolation and may instead be explained by factors including increased advection of oceanic heat to the Arctic region possibly insulated beneath a widening freshwater layer in the northern North Atlantic in conjunction with a shift in calcification season and/or depth habitat of *N. pachyderma* (sin).

1

Sub sea surface temperatures in the Polar North Atlantic during the Holocene: Planktic foraminiferal Mg/Ca temperature reconstructions

S. Aagaard-Sørensen[1*], K. Husum[1], M. Hald[1], T. Marchitto[2] and F. Godtliebsen[3]

[1] Department of Geology, University of Tromsø, 9037 Tromsø, Norway

[2] Department of Geological Sciences and Institute of Arctic and Alpine Research, University of Colorado, Campus Box 450, Boulder, Colorado 80309, USA

[3] Department of Mathematics and Statistics, University of Tromsø, 9037 Tromsø, Norway

[*]Author for correspondence: (e-mail: Steffen.Sorensen@uit.no)

Key words: Paleoceanography, Polar North Atlantic, Fram Strait, Atlantic water, Trace elements, sub SST reconstruction

Abstract

Holocene sea surface temperatures in the eastern Fram Strait are reconstructed based on Mg/Ca ratios measured on the planktic foraminifer *Neogloboquadrina pachyderma* (sin). The reconstructed sub sea surface temperatures ($sSST_{Mg/Ca}$) fluctuate markedly during the earliest Holocene at ~11.7–10.5 ka BP. This probably is in response to the varying presence of sea ice and deglacial melt water. Between ~10.5–7.9 ka BP the $sSST_{Mg/Ca}$ values are relatively high (~4°C) and more stable reflecting high insolation and intensified poleward advection of Atlantic water. After 7.9 ka BP the $sSST_{Mg/Ca}$ decline to an average of ~3°C throughout the mid-Holocene. These changes can be attributed to a combined effect of reduced poleward oceanic heat advection and a decline in insolation as well as a gradually increased influence of eastward migrating Arctic Water. The $sSST_{Mg/Ca}$ increase and vary between 2.1–5.8°C from ~2.7 ka BP to the present. This warming is in contrast to declining late Holocene insolation and may instead be explained by factors including increased advection of oceanic heat to the Arctic region possibly insulated beneath a widening freshwater layer in the northern North Atlantic in conjunction with a shift in calcification season and/or depth habitat of *N. pachyderma* (sin).

Introduction

In order to elucidate climate changes observed in Arctic environments today, it is necessary to improve the knowledge of long term natural climatic and oceanographic variations in the region (IPCC, 2007). At present, northward advection of Atlantic Water into the Nordic Seas and on to the Arctic is the main oceanic source of heat and salt for the Arctic Ocean (Schauer et al., 2004). During the Holocene other forcing mechanisms such as long-term orbital changes associated with insolation variability (Berger and Loutre, 1991), changes in atmospheric pressure systems resulting in displacement of primary wind patterns (North Atlantic Oscillation index) and alteration of Atlantic Water flux into the Nordic Seas (Hurrell, 51 1995; Nesje et al., 2001) have been suggested to have a large impact on climatic and oceanographic development in the Nordic Seas and the Arctic. Paleoceanographic variability, including temporal and spatial variation of Atlantic Water flux, temperature and salinity has previously been studied using a range of different proxies based on planktic foraminifera in the Nordic Seas during the Holocene. These include stable oxygen and carbon isotopes in foraminiferal tests (e.g. Bauch et al., 2001; Rasmussen et al., 2007) and distribution patterns of planktic foraminifera and transfer functions (e.g. Hald et al., 2007). Reconstructions of SST using transfer functions in the Arctic may be hampered by the databases representing modern conditions. The databases have a limited geographical coverage in the Arctic meaning that not all environmental gradients of the region are represented (e.g. Husum and Hald, 2012; Kucera et al., 2005). Moreover, stable oxygen isotopes recorded within foraminiferal calcite inherently reflect both the temperature and the $\delta^{18}O$ signal of ambient seawater (e.g. Shackleton, 1974). Therefore, additional proxies for paleo-SST are needed to elucidate cold-end temperature variability. Recent studies have utilized Mg/Ca ratios in planktic foraminifera to reconstruct sub sea surface temperatures ($sSST_{Mg/Ca}$) in the Fram Strait during the Late Glacial/Holocene transition and the late Holocene (Aagaard-Sørensen et al., submitted; Spielhagen et al., 2011). Here, we present the first record of $sSST_{Mg/Ca}$ from the entire Holocene in the high Arctic based on trace elements. A sediment core located under the present day inflow of Atlantic Water, carried within the West Spitsbergen Current (WSC), has been investigated (Figure 1A). Trace element analyses have been conducted on the planktic foraminifer *Neogloboquadrina pachyderma* (sin). Mg/Ca ratios were used to reconstruct sub surface water temperatures ($sSST_{Mg/Ca}$) representing the primary habitat depth and season of calcification for *N. pachyderma* (sin).

In addition, $\%CaCO_3$ and %TOC variations in the sediment were used to assess potential preservation changes of foraminiferal calcite in the record.

Oceanographic setting

Atlantic Water is advected northward in the North Atlantic Current (NAC; T>2°C, S>35) (Hopkins, 1991) and is transported into the Nordic Seas across the Iceland-Faroes-Scotland ridge systems at ~62°N (Hansen and Østerhus, 2000) (Figure 1A). At ca. 70°N the water mass bifurcates with one branch entering the SW Barents Sea while the other branch continues north along the west Barents Sea and Spitsbergen slopes as the West Spitsbergen Current (WSC) (Schauer et al., 2004) (Figure 1A). Atlantic Water (T: 3 to 7°C; S: 34.9 to 35.2) is carried by the WSC into the Arctic Ocean in the eastern part of the Fram Strait where it occupies the upper ~700 meters of the water column (Schauer et al., 2004; Walczowski et al., 2005) (Figure 1A). In the Fram Strait the Atlantic Water submerges at ~78°N and partly turns back to the south (Bourke et al., 1988) underneath the southward flowing East Greenland Current (Rudels et al. 2005) (Figure 1A). The remaining Atlantic Water disperses into several sub currents in the Arctic Ocean (Manley, 1995).

In the eastern Fram Strait modern temperatures of the surface mixed layer (0 to 25 m water depth) reach 8.2°C and a salinity up to 34.95 (August 2006) (Figure 1B). Below, from 25 to 550 m water depth Atlantic Water (T~4°C; S=35 to 35.15) occupies the water column and overlays Atlantic Intermediate Water (T>0°C; S~34.9). Deep Water is found from 900 m water depth (T<0°C, S~34.9).

Material and methods

Kastenlot core MSM05/5-712-2 (78˚54.94'N, 06˚46.03'E; 1488 m water depth; 894 cm length) was collected during a cruise with RV "Maria S. Merian" in August 2007 at the West Spitsbergen slope, eastern Fram Strait (Figure 1A).

Age model

The age model of MSM05/5-712-2 was constructed on the basis of 10 AMS ^{14}C dates and mean of the 2σ age ranges were used as tie points in the linear interpolation (Table 1, Figure

2). The AMS ^{14}C dates were carried out on planktic foraminiferal tests (*N. pachyderma* (sin)) from the upper 441 cm of the sediment core (Giraudeau (in prep); Werner et al., 2013). Radiocarbon dates were calibrated with Calib version 6.0 (Reimer et al., 2005; Stuiver et al., 2005) using the marine calibration curve Marine09 (Hughen et al., 2004; Reimer et al., 2009). The standard marine reservoir correction of 400 years (R) was used in all calibrations. The local reservoir age ($\Delta R=151\pm51$) from Magdalenefjorden, Svalbard was used in the calibration (Mangerud et al., 2006; Mangerud and Gulliksen, 1975) (Table 1). All calibrated ages are an expression of years before present (1950). The Younger Dryas/Holocene boundary (11.75 ka BP) used on figures follows Walker et al. (2009).

Trace element analysis and contaminants

The sediment core was sub sampled in 1 cm thick slices, and then freeze dried and wet sieved trough 1 mm, 100 µm and 63 µm mesh sizes. Trace element analysis was performed on the planktic foraminifer *Neogloboquadrina pachyderma* (sinistral coiling) (ca. 50 tests/sample) and the trace element ratios Mg/Ca, Mn/Ca, Fe/Ca, and Al/Ca were measured (Figure 3 and 4). Tests were picked at 2 cm and 3 cm resolution in the upper part (0 to 210 cm) and lower part (210 to 441 cm) of the sediment core, respectively, resulting in a temporal resolution of ~36 to 120 yr/sample. Given that partial dissolution and contamination of tests can bias the trace element analysis, dirty and sediment filled tests or tests visibly influenced by dissolution (i.e. broken tests or tests with missing chambers) were avoided. Furthermore, tests were picked within a relatively narrow size range, with minimum and maximum length of the tests ranging from ca. 225 to 290 µm, to reduce size dependent bias on the Mg/Ca measurements (Elderfield et al., 2002). Prior to analysis the foraminiferal tests were crushed and reductively (anhydrous hydrazine) and oxidatively (H_2O_2) cleaned (Boyle and Keigwin, 1985; Boyle and Rosenthal, 1996). Subsequently the samples were analyzed by magnetic-sector single collector ICP-MS, on a Thermo-Finnigan Element2 at the Litmann laboratory, University of

Colorado operating with a long-term 1σ precisions of 0.54% for Mg/Ca measurements (Marchitto, 2006). Replicate analysis was carried out for approximately every 30 samples. The average reproducibility of sample splits was ±0.039 mmol/mol (n=4) in regards to Mg/Ca which on average is below <5% difference between duplicate measurements (Figure 4C). Fe, Al and Mn are tracers of contaminating phases that might bias the Mg/Ca ratios measured in foraminiferal calcite (Barker et al., 2003). Fe and Al are tracers of detrital material contamination (silicate minerals) and Mn is tracer of secondary diagenetic Mn-rich carbonate coating (Boyle, 1983). Weak correlation between Mg and Fe (R^2~0.26) and Mn (R^2~0.21) is observed whereas Al shows no significant correlation to Mg (R^2~0.03) (Figure 3A, B, C). Samples with >100 μmol/mol of Fe, Al and Mn (Barker et al., 2003) in addition to samples with <5 μg $CaCO_3$ recovery (Marchitto, 2006) were omitted (Figure 4C).

Water temperature reconstructions

Temperature of the ambient sea water is considered to be the primary controlling factor on Mg/Ca ratios recorded in foraminiferal calcite (Elderfield and Ganssen, 2000; Lea et al., 1999; Nürnberg et al., 1996). The thermodynamic control on the Mg uptake into foraminiferal calcite shows positive exponential relation between temperature and Mg uptake which approximates a linear relationship at narrow temperature ranges (Elderfield and Ganssen, 2000; Kozdon et al., 2009; Kristjánsdóttir et al., 2007).

Sub sea surface temperatures ($sSST_{Mg/Ca}$) were calculated using Mg/Ca ratios and the species specific (*N. pachyderma* (sin)) linear equation of Kozdon et al. (2009) (Figure 4, 5, 6):

$$\text{Mg/Ca (mmol mol}^{-1}) = 0.13\ (\pm 0.037) * T + 0.35\ (\pm 0.17) \quad \text{(Eq. 1)}$$

This equation is based on cross calibrated Mg/Ca and $\delta^{44/40}$ Ca proxy signals of *N. pachyderma* (sin) from Nordic Sea core top samples and produces reliable $sSST_{Mg/Ca}$ estimates at temperatures above ~3°C (Kozdon et al., 2009). It must be cautioned that the equation is based on samples that have not undergone the reductive cleaning step (Kozdon et al., 2009).

SiZer analysis

SiZer (Significance of Zero Crossings of the Derivative) analysis described by Chaudhuri and Marron (1999) was performed on the $sSST_{Mg/Ca}$ data to reveal significant features in the proxy record (Figure 6C). The analysis has previously been applied to Arctic paleo proxy records to reveal significant features at particular levels of resolution and eliminating insignificant natural variability (e.g. Hald et al., 2004; Wilson et al., 2011). The method assumes that individual values are independent random variables. The analyses smooth the data from minimum to maximum resolution and generate a SiZer map which examines the data across a range of resolutions (bandwidth, h) and uses color codes to classify the derivatives of the smoothed data as significantly decreasing, increasing or exhibiting no significant change (Figure 6C).

Results

The record of Mg/Ca ratios measured on *N. pachyderma* (sin) has an average value of 0.809 mmol/mol ($n = 152$; $1\sigma = 0.11$) corresponding to an average temperature of 3.5°C (Figure 4C, D). Measurements of Mg/Ca ratios showing possible sample contamination have been removed from the record (Figure 4C, D).

During the earliest Holocene the $sSST_{Mg/Ca}$ values are relatively high and fluctuating between 1.9 and 5.2°C (Figure 4D). Between ~10.5–7.9 ka BP the $sSST_{Mg/Ca}$ are relatively high values with an average of ~4°C (Figure 4D). After ~7.9 ka BP the $sSST_{Mg/Ca}$ decline rapidly to <3°C. The mid Holocene is characterized by two cold periods, ~7.9–6 ka BP and 5.2–2.7 ka BP, with an average $sSST_{Mg/Ca}$ of ~3°C bracket an interval with slightly elevated $sSST_{Mg/Ca}$ (~3.5°C). During the Late Holocene the $sSST_{Mg/Ca}$ values gradually increase towards the present. The highest values averaging ~5°C are recorded after ~1 ka BP (Figure 4D).

The SiZer analysis identifies a multi-millennial $sSST_{Mg/Ca}$ decline from ~11.7– 6 ka BP with a significant sub-millennial decrease around 7.9 ka BP (Figure 6C). From ~6–3 ka BP no significant change is observed. A significant warming on multi decadal to multi millennial time scale is initiates at ~3 ka BP (Figure 6C).

Discussion

Assessment of reconstructed $sSST_{Mg/Ca}$ and calcium carbonate preservation state

During analysis the foraminiferal calcite undergoes reductive and oxidative cleaning (see material and methods for details). The reductive cleaning decreases the Mg/Ca ratio by up to 10-15 % potentially lowering the reconstructed $sSST_{Mg/Ca}$ (Barker et al., 2003).

Comparison of reconstructed $sSST_{Mg/Ca}$ with summer $sSST_{SIMMAX}$ based on foraminiferal distribution patterns in the same core (Werner et al., 2013) shows similar temperature ranges of 1.9 to 5.8°C and 0.9 to 6.1°C, respectively (Figure 5C). It should be noted that below the lower limit of sensitivity for Eq. 1 (< 3°C) (Kozdon et al., 2009) the Mg/Ca method does not reproduce comparable low temperature estimates as the $sSST_{SIMMAX}$ (Werner et al., 2013) (Figure 5C). In order to estimate the potential impact of Mg loss during reductive cleaning (Barker et al., 2003) we artificially increased the Mg/Ca ratio by 15% in figure 5C. The resulting $sSST_{Mg/Ca+15\%}$ calculated using Eq. 1 (Kozdon et al., 2009) shows increases of 0.7 to 1.3°C generally producing higher estimates than $sSST_{SIMMAX}$ (Figure 5C). Therefore the potential Mg loss during the reductive cleaning (i.e. lower reconstructed temperature) in our record is considered of minor importance.

Further, Mg/Ca ratios were measured in core-top *N. pachyderma* (sin) (Core MSM5/5-712-1) obtained from same core location as MSM5/5-712-2 (Speilhagen et al., 2011) (Figure 1). The material underwent the same cleaning procedure as applied in the present study (Spielhagen et al., 2011). The core-top $sSST_{Mg/Ca}$ is ~5.1°C when calculated using the temperature equation of Elderfield & Ganssen (2000) (Speilhagen et al., 2011) (Figure 5B) and ~3.7°C when recalculated using Eq.1 (Figure 5B) (Kozdon et al., 2009). Both values are within or close to the modern temperature range (August 2009) observed at the main *N. pachyderma* (sin) habitat depth of 50-200 m water depth (Figure 1B, 5C). These findings further show that any potential Mg loss during cleaning procedures is of minor importance for the reconstructed temperatures.

Studies have shown that dissolution of calcium carbonate is a prominent feature in paleo-records from the Fram Strait especially after ~8 ka BP (Bauch et al., 2001; Rasmussen et al., 2007; Zamelczyk et al., 2012). Post mortem dissolution of foraminiferal calcite may preferentially remove Mg rich parts from foraminiferal tests and consequently bias Mg/Ca ratio based temperature reconstructions towards lower, colder values (Brown and Elderfield, 1996; Johnstone et al., 2011; Rosenthal et al., 2000). In order to minimize the risk of measuring on material influenced by dissolution only the most pristine test were picked for trace element analysis (see material and methods section for more details). Further, %$CaCO_3$ and %TOC variations in the sediment can be used to tentatively assess potential preservation changes of foraminiferal calcite in the record (Figure 4A, B). The sediment holds low content of $CaCO_3$ (≤5 wt.%) and high content of total organic carbon (%TOC) prior to ~10 ka BP (Aagaard et al., submitted) (Figure 4A, B) which may suggest potential post-depositional dissolution due to respiratory release of CO_2 and decrease of pore water pH during organic material degradation within the sediment (e.g. Archer et al., 1989; Emerson and Bender, 1981; Huber et al., 2000). After ~10 ka BP to the present high %$CaCO_3$ and low %TOC generally indicates good preservation potential, apart from the mid-Holocene (~6–3 ka BP) where relatively low %$CaCO_3$ and moderate %TOC content has been recorded (Müller at al., 2012). This could indicate preservation problems although to a lesser extent than during the earliest Holocene (4 A,B). To what extent preservation/dissolution has influenced the Mg/Ca ratios recorded by *N. pachyderma* (sin) is not possible to quantify from the present set of proxies. However, it cannot be excluded that the preservation changes of foraminiferal tests during the Holocene may have influenced the reconstructed $sSST_{Mg/Ca}$ values.

Holocene sSST variability

Based on the $sSST_{Mg/Ca}$ record and significant changes identified by the SiZer analysis the paleorecord of core MSM5/5-712-2 can be divided into three intervals: The relatively warm early (11.7–7.9 ka BP), cold mid (7.9–2.7 ka BP) and warm late (2.7–0.3 ka BP) Holocene (Figure 4, 6).

Early Holocene (11.7–7.9 ka BP)

Previous studies from the Fram Strait have shown that the early Holocene was characterized by a strong influence of sea ice, icebergs and glacial melt water prior to ~10.5 ka BP (Aagaard-Sørensen et al., submitted; Ebbesen et al., 2007; Rasmussen et al., 2007; Ślubowska-Woldengen et al., 2005). The low $sSST_{Mg/Ca}$ recorded at ~11–11.3 ka BP (represented by 3 data points) (Figure 6D) possibly reflects a cooling associated with the brief but distinct climatic event, the Preboreal Oscillation (PBO). The PBO has been documented in both marine and terrestrial records in and around the Nordic Seas (e.g. Björck et al., 1997; Hald and Hagen, 1998; Husum and Hald, 2002; Rasmussen, SO et al., 2007). The PBO has been attributed to increased deglacial melt water fluxes into the Nordic and Arctic Seas resulting in hampered heat transport via the North Atlantic conveyor and enhanced sea ice export into the Fram Strait (Fisher et al., 2002; Hald and Hagen 1998).

In the present record the highest early Holocene $sSST_{Mg/Ca}$ (average ~4°C) is found between ~10.5 to 7.9 ka BP (Figure 6D). A marked summer $sSST_{Mg/Ca}$ increase initiated at ~11 ka BP and subsequent peak values between ~10.5–8.7 ka BP has been recorded along the Barents

249 Sea and West Spitsbergen slopes via planktic foraminiferal transfer functions ($sSST_{Transfer}$)
250 (Ebbesen et al., 2007; Hald et al., 2007; Husum and Hald, 2012; Sarnthein et al., 2003)
251 (Figure 6F, G). The summer sSST increase along the West Spitsbergen slope is part of a
252 south to north time-transgressive development in the Nordic Seas, where the remnant cold
253 water and sea ice gradually was displaced by Atlantic Water (Hald et al., 2007).
254 Risebrobakken et al. (2011) argue that strong melt water discharge resulted in weak
255 ventilation of the Nordic Seas until 11 ka BP. A buildup of an Atlantic subsurface reservoir
256 of heat and salt eventually resulted in rejuvenation of strong and deep overturning circulation
257 and intensified early Holocene northward heat advection into the Nordic Seas peaking at 10
258 ka BP (Risebrobakken et al., 2011). Predominantly positive North Atlantic Oscillation (NAO)
259 index values reconstructed by Nesje et al. (2001) also support stronger northward advection
260 of Atlantic Water during the early Holocene (Hurrell, 1995). The NAO index is defined as
261 the atmospheric pressure difference between Iceland and the Azores with positive index
262 values indicating a larger pressure difference, resulting in stronger westerlies which increase
263 wind driven Atlantic Water influx to the Nordic Seas (Hurrell, 1995).
264 Within the significant multi-millennial $sSST_{Mg/Ca}$ decline observed throughout the early part
265 of the record a faster multi-centennial decline is observed following the relatively high early
266 Holocene $sSST_{Mg/Ca}$ from ~10.5 to 7.9 ka BP (Figure 6C, D). An early to middle Holocene
267 cooling has been recorded in different proxy records in the Nordic Sea including distribution
268 patterns of diatoms (Birks and Koç, 2002; Koç et al., 1993) and benthic and planktic
269 foraminifera (Hald and Aspeli, 1997; Hald et al., 2004; Ebbesen et al., 2007; Knudsen et al.,
270 2004; Rasmussen et al., 2007; Werner et al., 2013). The observed pattern could be a
271 reflection of the high and declining summer insolation (Berger and Loutre, 1991) (Figure
272 6A). However, studies suggest that insolation changes primarily influence the uppermost part
273 (summer mixed layer down to ~20-40 m water depth) of the water column (e.g. Andersson et

al., 2009; Risebrobakken et al., 2011). Since our data are derived from the subsurface dwelling *N. pachyderma* (sin) (Kozdon et al., 2009; Simstich et al., 2003; Volkmann, 2000) the observed $sSST_{Mg/Ca}$ decline (Figure 6C, D) probably only partly reflects the declining insolation forcing (Berger and Loutre, 1991) (Figure 6A), but also indicates a gradual reduction in northbound Atlantic Water transport as suggested by Risebrobakken et al. (2011).

Mid Holocene (7.9–2.7 ka BP)

This period is characterized by the lowest $sSST_{Mg/Ca}$ recorded by *N. pachyderma* (sin). The SiZer analysis identifies no significant changes apart from the overall multi-millennial early Holocene decline ending at ~6 ka BP and initial increase identified at ~3 ka BP (Figure 6C, D). This cold interval may be partly driven by continued decrease in insolation (Berger and Loutre, 1991) (Figure 6A) and/or weakened poleward advection of Atlantic Water as indicated by the frequently negative phase of the NAO during the mid-Holocene (Hurrell, 1995; Nesje et al., 2001). Hald et al. (2007) suggest that increased influence of Arctic Water, in response to lowered insolation and reduced oceanic heat advection may have caused the mid Holocene cooling and low $sSST_{Transfer}$ along the Barents Sea - and west Spitsbergen slopes (Ebbesen et al., 2007; Husum and Hald, 2012; Sarnthein et al., 2003) (Figure 6F, G). During the early part of the mid-Holocene, before ~7 ka BP, relatively high phytoplankton-derived biomarker content points to high surface water productivity in the eastern Fram Strait (Müller et al., 2012). This suggests continued influence of the still relatively high insolation on the surface water mass (Müller et al., 2012). However, within the sub-surface water masses the reduced $sSST_{Mg/Ca}$ values suggest an increased influence of Arctic water almost 900 years earlier from ~7.9 ka BP (Figure 6D). After ~7 ka BP, continued low $sSST_{Mg/Ca}$ recorded by *N. pachyderma* (sin) (Figure 6D) are in agreement with weakened poleward advection of Atlantic Water (Hald et al., 2007; Risebrobakken et al., 2011) and cooling of the

299 surface water mass resulting in lowered productivity and extension of (winter/spring) sea ice (Müller et al., 2012). Faunal distributions in core MSM5/5-712-2 indicate relatively strong Atlantic Water advection until ~5.2 ka following a slight weakening after ~8 ka BP (Werner et al., 2013). Fluctuating $sSST_{SIMMAX}$ values during this period, including cooling events at 6.9 and 6.1 ka BP, are also tied to repeated advances and retreats of the sea-ice margin connected to south east movement of the Arctic Front separating Atlantic and Arctic waters masses (Werner et al., 2013) (Figure 6E).

Prevailing cold conditions seen in the $sSST_{Mg/Ca}$ and $sSST_{SIMMAX}$ reconstructions and supported by predominantly heavy $\delta^{18}O$ values measured on *N. pachyderma* (sin) occur from 5.2 to 2.7 ka BP (Werner et al., 2013) (Figure 5A, 6D, E). In combination with increased IP_{25} concentrations (sea ice biomarker) the data indicate more severe sea ice conditions and stronger influence from Arctic water during this period (Müller et al., 2012; Werner et al., 2013) (Figure 6B). The overall similar trend seen in the $sSST_{Mg/Ca}$ and $sSST_{SIMMAX}$ suggests that both reconstructions reflect summer conditions (Figure 6D, E). The lower amplitude observed in the $sSST_{Mg/Ca}$ may be related to calcification depth of *N. pachyderma* (sin) as the $sSST_{SIMMAX}$ reconstructs temperatures for 50 m water depth whereas $sSST_{Mg/Ca}$ probably reflects a somewhat deeper water depth. The modern main habitat depth of *N. pachyderma* (sin) is 50 to 200 m water depth in Fram Strait (Volkmann, 2000). At the ice margin and in areas affected by warm Atlantic water masses the main habitat center at ~100 m water depth (Volkmann, 2000). In ice covered and cold Polar Water masses the average habitat depth lies between 50–100 m (Volkmann, 2000).

Late Holocene (2.7–0.3 ka BP)

The late Holocene is characterized by significantly increasing $sSST_{Mg/Ca}$ toward the present (Figure 6C, D). The highly fluctuating $sSST_{Mg/Ca}$ signal has values intermittently higher than those recorded during the early Holocene (Figure 6D). During this time, more severe and gradually increasing ice coverage in the eastern Fram Strait has been inferred from elevated sediment IP_{25} and IRD contents (Müller et al., 2012) (Figure 6B). In addition, in-phase fluctuations of IP_{25} and phytoplankton marker contents have been linked to periods of a rapidly advancing and retreating sea ice margin (Müller et al., 2012). The late Holocene expansion of sea ice and general cooling of the surface water masses have also been observed in other sea surface proxy records from the Nordic Seas (e.g. Andersen et al., 2004; Koç et al., 1993; Koç Karpuz and Jansen, 1992) and is in line with the low and declining Northern hemispheric insolation (Berger and Loutre, 1991) (Figure 6A). However, the present $sSST_{Mg/Ca}$ reconstruction and other subsurface proxy records derived from cores situated under the axis of northward Atlantic Water flow in the Nordic Seas register a late Holocene temperature increase that is in contrast to the reduced insolation forcing (Andersson et al., 2009; Dolven et al., 2002; Ebbensen et al., 2007; Risebrobakken et al., 2003; Sarnthein et al., 2003; Werner et al., 2013) (Figure 6E-H). Increased poleward Atlantic Water advection as indicated by the predominantly positive phase of the NAO after ~2 ka BP (Nesje et al., 2001; Olsen et al., 2012) may partially explain the observed late Holocene subsurface warming (Figure 6D). Furthermore, freshening and cooling of the surface waters due to melting of sea ice and/or icebergs could have resulted in migration of *N. pachyderma* (sin) to a deeper and possibly warmer part of the water column where conditions were more favorable (Kozdon et al., 2009; Simstich et al., 2003). A gradual migration *N. pachyderma* (sin) to deeper, less ventilated water masses is inferred by Werner et al. (2013) on the basis of gradually decreasing $\delta^{13}C$ values after ~3.5 ka BP. Werner et al. (2013) speculate that the light $\delta^{13}C$ values observed in MSM5/5-712-2 and other records in the northern North Atlantic indicate a wider distribution of a sea-ice derived freshwater layer in the Nordic Seas during the late Holocene. We further speculate that northbound Atlantic water masses, as a consequence of a widespread and possibly expanding melt water layer, could have submerged further south thus becoming gradually more insulated during the late Holocene. This could partially explain the increasingly warmer $sSST_{Mg/Ca}$ observed in the present record (Figure 6D) and trend towards less ventilated lighter $\delta^{13}C$ observed by Werner et al. (2013). Additionally, the low insolation (Berger and Loutre, 1991) (Figure 6A) and the increasingly severe sea ice conditions in the eastern Fram Strait (Müller et al., 2012) (Figure 6B) may have facilitated a shift in the growing season for phytoplankton and foraminifera towards a gradually warmer part of the season (e.g. Farmer et al., 2008). In the Arctic Ocean the highest production and thus main calcification season of *N. pachyderma* (sin) is observed in August and is likely linked to phytoplankton blooms (Kohfeld et al., 1996; Volkmann, 2000).

Conclusions

Mg/Ca element ratios measured on *N. pachyderma* (sin) have been used to reconstruct Holocene sub sea surface temperatures ($sSST_{Mg/Ca}$) on the West Spitsbergen Slope, eastern Fram Strait.

A tentative assessment of foraminiferal calcite preservation based on $\%CaCO_3$ and %TOC contents in the sediment may suggest preservation problems prior to ~10 ka BP and possibly also from ~6–3 ka BP.

The fluctuating $sSST_{Mg/Ca}$ observed during the earliest part of the early Holocene can probably be associated with variable paleoceanographic conditions in response to lingering sea ice, ice berg and melt water presence. During the early Holocene from ~10.5–7.9 ka BP $sSST_{Mg/Ca}$ reach an average value of ~4°C. These relatively high values probably reflect a strong northward oceanic heat advection in combination with high insolation forcing.

A significant long-term (multi-millennial) decrease in $sSST_{Mg/Ca}$ was identified throughout the early Holocene with steeper (sub-millennial) decline recorded at ~9–7 ka BP. The coldest $sSST_{Mg/Ca}$ values observed in the current record, with values averaging ~3°C, were recorded in two periods from ~7.7–6 and ~5.2–2.7 ka BP. This cooling during the mid-Holocene may be attributed to an increased influence of eastward migrating Arctic Water in response to hampered northward oceanic heat advection into the Fram Strait and decreasing insolation forcing.

During the late Holocene, after ~2.7 ka BP, $sSST_{Mg/Ca}$ significantly increased as shown by the SiZer analysis. The $sSST_{Mg/Ca}$ reached an average value of ~5°C during the last 1000 year. This $sSST_{Mg/Ca}$ increase can possibly be linked to a stronger advection of Atlantic Water as supported by positive NAO index values combined with an insulating effect of a widespread melt water layer in the northern North Atlantic. The high $sSST_{Mg/Ca}$ values during the late Holocene potentially also could be partly explained by a shift in calcification season and/or change of depth habitat for *N. pachyderma* (sin).

Acknowledgements

This work has been carried out within the framework of the International Polar Year project "Arctic Natural Climate and Environmental Changes and Human Adaption: From Science to Public Awareness" (SciencePub) funded by the Research Council of Norway and the Trainee School in Arctic Marine Geology & Geophysics, University of Tromsø and the Norwegian Research Council. The core was collected onboard the R/V "Maria S. Merian" during the MSM05/5b expedition led by Dr. Gereon Budeus, Alfred Wegener Institute. Patrick Cappa assisted the laboratory work at INSTAAR, University of Colorado. Jan Petter Holm prepared the area map. Two anonymous reviewers, R. Kozdon and K. Zamelczyk gave valuable comments and suggestions. To these institutions and persons we offer our sincere thanks.

References

Aagaard-Sørensen, S, Husum K, Werner K, et al. (Submitted) A Late glacial-early Holocene multiproxy record, Fram Strait, Polar North Atlantic. *Marine Geology*

Andersen C, Koc N and Moros M (2004) A highly unstable Holocene climate in the subpolar North Atlantic: evidence from diatoms. *Quaternary Science Reviews* 23: 2155–2166.

Andersson C, Pausata FSR, Jansen E et al. (2009) Holocene trends in the foraminifer record from the Norwegian Sea and the North Atlantic Ocean. *Climate of the Past Discussions* 5: 2081–2113.

Archer D, Emerson S, and Reimers C (1989) Dissolution of calcite in deep-sea sediments:pH and O_2 microelectrode results. *Geochimica et Cosmochimica Acta* 531: 2831–2845.

Barker S, Greaves M, and Elderfield H (2003) A study of cleaning procedures used for foraminiferal Mg/Ca paleothermometry. *Geochemistry, Geophysics, Geosystems* 4: DOI: 10.1029/2003gc000559.

Bauch HA, Erlenkeuser H, Spielhagen RF et al. (2001) A multiproxy reconstruction of the evolution of deep and surface waters in the subarctic Nordic seas over the last 30,000 yr. *Quaternary Science Reviews* 20: 659–678.

Berger A and Loutre MF (1991) Insolation values for the climate of the last 10 million years. *Quaternary Science Reviews* 10: 297–317.

Birks CJA and Koç N (2002) A high-resolution diatom record of late-Quaternary sea-surface temperatures and oceanographic conditions from the eastern Norwegian Sea. *Boreas* 31**:** 323–344.

Björck S, Rundgren M, Ingólfsson Ó and Funder S (1997) The Preboreal oscillation around the Nordic Seas: terrestrial and lacustrine responses. *Journal of Quaternary Science* 12: 455-465.

Bourke RH, Weigel AM and Paquette RG (1988) The Westward Turning Branch of the West Spitsbergen Current. *Journal of Geophysical Research* 93: 14065-14077.

Boyle EA (1983) Manganese carbonate overgrowths on foraminifera tests. *Geochimica et Cosmochimica Acta* 47: 1815–1819.

Boyle EA and Keigwin LD (1985) Comparison of Atlantic and Pacific paleochemical records for the last 215,000 years: changes in deep ocean circulation and chemical inventories. *Earth and Planetary Science Letters* 76: 135-150.

Boyle EA and Rosenthal Y (1996) Chemical hydrography of the South Atlantic during the Last Glacial Maximum: Cd and $\delta^{13}C$. In: G. Wefer et al. (eds) *The South Atlantic: Present and Past Circulation*. New York: Springer-Verlag, pp.423–443.

Brown SJ and Elderfield H (1996) Variations in Mg/Ca and Sr/Ca ratios of planktonic foraminifera caused by postdepositional dissolution: Evidence of shallow Mg-dependent dissolution. *Paleoceanography* 11(5): 543-551.

Chaudhuri P and Marron S (1999) SiZer for exploration of sturctures in curves. *Journal of the Amerikan Statistical Association* 94: 807-823.

Dolven JK, Cortese G and Bjørklund KR (2002) A high-resolution radiolarian-derived paleotemperature record for the Late Pleistocene-Holocene in the Norwegian Sea. *Paleoceanography* 17(4), 1072. DOI:10.1029/2002pa000780.

Ebbesen H, Hald M and Eplet TH (2007) Late glacial and early Holocene climatic oscillations on the western Svalbard margin, European Arctic. *Quarternary Science Reviews* 26: 1999-2011.

Elderfield H and Ganssen GM (2000) Past temperature and $\delta^{18}O$ of surface ocean waters inferred from foraminiferal Mg/Ca ratios. *Nature* 405: 442–445.

Elderfield H, Vautravers M and Cooper M (2002) The relationship between shell size and Mg/Ca, Sr/Ca, $\delta^{18}O$, and $\delta^{13}C$ of species of planktonic foraminifera. *Geochemistry, Geophysics, Geosystems* 3(8), DOI:10.1029/2001gc000194.

Emerson S and Bender M (1981) Carbon fluxes at the sediment-water interface of the deep-sea: calcium carbonate preservation. *Journal of Marine Research* 39: 139–162.

Farmer EJ, Chapman MR and Andrews JE (2008) Centennial-scale Holocene North Atlantic surface temperatures from Mg/Ca ratios in *Globigerina bulloides*. *Geochemistry, Geophysics, Geosystems* 9, DOI:10.1029/2008GC002199.

Fisher TG, Smith DG and Andrews JT (2002) Preboreal oscillation caused by a glacial Lake Agassiz flood. *Quaternary Science Reviews* 21: 873–878.

Giraudeau J (in prep) EPOC (University Bordeaux 1/CNRS) within the framework of an ongoing IFM-GEOMAR / EPOC collaboration.

Hald M and Aspeli R (1997) Rapid climatic shifts of the nothern Norwegian Sea during the last deglaciation and the Holocene. *Boreas* 26: 15-28.

Hald M and Hagen S (1998) Early preboreal cooling in the Nordic Sea region triggered by meltwater. *Geology* 26**:** 615-618..

Hald M, Ebbesen H, Forwick M et al. (2004) Holocene paleoceanography and glacial history of the West Spitsbergen area, Euro-Arctic margin. *Quaternary Science Reviews* 23: 2075-2088.

Hald M, Andersson C, Ebbesen H et al. (2007) Variations in temperature and extent of Atlantic Water in the northern North Atlantic during the Holocene. *Quaternary Science Reviews* 26: 3423-3440.

Hansen B and Østerhus S (2000) North Atlantic-Nordic Seas exchanges. *Progress In Oceanography* 45: 109-208.

Hopkins TS (1991) The GIN Sea--A synthesis of its physical oceanography and literature review 1972-1985. *Earth-Science Reviews* 30(3-4): 175-318.

Huber R, Meggers H, Baumann KH and Henrich R (2000) Recent and Pleistocene carbonate dissolution in sediments of the Norwegian–Greenland Sea. *Marine Geology* 165(1–4): 123-136.

Hughen KA, Baillie MGL, Bard E et al. (2004) Marine04 marine radiocarbon age calibration, 0-26 cal kyr BP. *Radiocarbon* 46: 1059-1086.

Hurrell JW (1995) Decadal Trends in the North Atlantic Oscillation Regional Temperatures and Precipitation. *Science* 269**:** 676-679.

Husum K and M Hald (2002) Early Holocene cooling events in Malangenfjord and the adjoining shelf, north-east Norwegian Sea. *Polar Research* 21(2): 267-274.

Husum K and M Hald (2012) Arctic planktic foraminiferal assemblages: Implications for subsurface temperature reconstructions. *Marine Micropaleontology* 96–97(0): 38-47.

Intergovernmental Panel on Climate Change (2007) *Climate Change 2007: The Physical Science Basis. Contribution of Working Group I to the Fourth Assessment Report of the Intergovernmental Panel on Climate Change*. Cambridge University Press.

Johnstone HJH, Yu J, Elderfield H and Schulz M (2011) Improving temperature estimates derived from Mg/Ca of planktonic foraminifera using X-ray computed tomography-based dissolution index, XDX. *Paleoceanography* 26(1): PA1215, DOI: 10.1029/2009pa001902.

Knudsen KL, Jiang H, Jansen E et al. (2004) Environmental changes off North Iceland during the deglaciation and the Holocene: foraminifera, diatoms and stable isotopes. *Marine Micropaleontology* 50: 273-305.

Koç Karpuz N and Jansen E (1992) A high-resolution diatom record of the last deglaciation from the SE Norwegian Sea: Documentation of rapid climatic changes. *Paleoceanography* 7**:** 499–520.

Koç N, Jansen E and Haflidason H (1993) Paleoceanographic reconstructions of surface ocean conditions in the Greenland, Iceland and Norwegian seas through the last 14 ka based on diatoms. *Quaternary Science Reviews* 12: 115-140.

Kohfeld KE, Fairbanks RG, Smith SL et al. (1996) *Neogloboquadrina pachyderma* (sinistral coiling) as paleoceanographic tracers in polar oceans: evidence from Northeast Water Polynya plankton tows, sediments traps, and surface sediments. *Paleoceanography* 11: 679–699.

Kozdon R, Eisenhauer A, Weinelt M et al. (2009) Reassessing Mg/Ca temperature calibrations of *Neogloboquadrina pachyderma* (sinistral) using paired $\delta^{44/40}Ca$ and Mg/Ca measurements. *Geochemistry Geophysics Geosystems* 10: Q03005, DOI: 10.1029/2008GC002169

Kristjánsdóttir GB, Lea DW, Jennings AE et al. (2007) New spatial Mg/Ca-temperature calibrations for three Arctic, benthic foraminifera and reconstruction of north Iceland shelf temperature for the past 4000 years. *Geochemistry Geophysics Geosystems* 8: Q03P21, DOI: 10.1029/2006GC001425

Kucera M, Weinelt M, Kiefer T et al. (2005) Reconstruction of sea-surface temperatures from assemblages of planktonic foraminifera: multi-technique approach based on geographically constrained calibration data sets and its application to glacial Atlantic and Pacific Oceans. *Quaternary Science Reviews* 24: 951-998.

Lea DW, Mashiotta TA and Spero HJ (1999) Controls on magnesium and strontium uptake in planktonic foraminifera determined by live culturing. *Geochimica et Cosmochimica Acta* 63: 2369-2379.

Mangerud J and Gulliksen S. (1975) Apparent radiocarbon ages of Recent marine shells from Norway, Spitsbergen, and Arctic Canada. *Quaternary Research* 5: 263-273.

Mangerud J, Bondevik S, Gulliksen S et al. (2006) Marine ^{14}C reservoir ages for 19th century whales and molluscs from the North Atlantic. *Quaternary Science Reviews* 25: 3228-3245.

Manley TO (1995) Branching of Atlantic Water within the Greenland-Spitsbergen passage: An estimate of recirculation. *Journal of Geophysical Research* 100: 20627-20634.

Marchitto TM (2006) Precise multielemental ratios in small foraminiferal samples determined by sector field ICP-MS. *Geochemistry Geophysics Geosystems* 7: Q05P13, DOI:10.1029/2005GC001018.

Marnela M, Rudels B, Olsson KA et al. (2008) Transports of Nordic Seas water masses and excess SF6 through Fram Strait to the Arctic Ocean. *Progress In Oceanography* 78(1): 1-11.

Müller J, Werner K, Stein R et al. (2012) Holocene cooling culminates in sea ice oscillations in Fram Strait. *Quaternary Science Reviews* 47: 1-14.

Nesje A, Matthews JA, Dahl SO et al. (2001) Holocene glacier fluctuations of Flatebreen and winter-precipitation changes in the Jostedalsbreen region, western Norvay, based on glaciolacustrine sediment records. *The Holocene* 11: 267-280. DOI:10.1191/095968301669980885

Nürnberg D, Bijma J and Hemleben C (1996) Assessing the reliability of magnesium in foraminiferal calcite as a proxy for water mass temperatures. *Geochimica et Cosmochimica Acta 60*(5): 803-814.

Olsen J, Anderson NJ and Knudsen MF (2012) Variability of the North Atlantic Oscillation over the past 5,200 years. *Nature Geoscience* 5*:* 808–812*,* DOI:10.1038/ngeo1589

Rasmussen SO, Vinther BM, Clausen HB and Andersen KK (2007) Early Holocene climate oscillations recorded in three Greenland ice cores. *Quaternary Science Reviews* 26: 1907-1914.

Rasmussen TL, Thomsen E, Ślubowska MA et al. (2007) Paleoceanographic evolution of the SW Svalbard margin (76^0N) since 20,000 ^{14}C yr BP. *Quaternary Research* 67: 100-114.

Reimer P, Baillie M, Bard E et al. (2005) IntCal04 Terrestrial Radiocarbon Age Calibration, 0-26 Cal Kyr BP. *Radiocarbon* 46: 1029-1058.

Reimer P, Baillie M, Bard E et al. (2009) IntCal09 and Marine09 Radiocarbon Age Calibration Curves, 0–50,000 Years cal BP. *Radiocarbon* 51: 1111–1150.

Risebrobakken B, Jansen E, Andersson C et al. (2003) A high-resolution study of Holocene paleoclimatic and paleoceanographic changes in the Nordic Seas. *Paleoceanography* 18: 1017-1034.

Risebrobakken B, Dokken T, Smedsrud LH et al. (2011) Early Holocene temperature variability in the Nordic Seas: The role of oceanic heat advection versus changes in orbital forcing. *Paleoceanography* 26(4): PA4206, DOI:10.1029/2011pa002117.

Rosenthal Y, Lohmann GP, Lohmann KC and Sherrell RM (2000) Incorporation and preservation of Mg in *Globigerinoides sacculifer*: implications for reconstructing the temperature and $^{18}O/^{16}O$ of seawater. *Paleoceanography* 15(1): 135-145.

Rudels B, Björk G, Nilsson J et al. (2005) The interaction between waters from the Arctic Ocean and the Nordic Seas north of Fram Strait and along the East Greenland Current: results from the Arctic Ocean-02 Oden expedition. *Journal of Marine Systems* 55(1-2): 1-30.

Sarnthein M, Van Kreveld S, Erlenkeuser H et al. (2003) Centennial-to-millennial-scale periodicities of Holocene climate and sediment injections off the western Barents shelf, 75^oN. *Boreas* 32: 447-461.

Schauer U, Fahrbach E, Osterhus S and Rohardt G (2004) Arctic warming through the Fram Strait: Oceanic heat transport from 3 years of measurements. *Journal of Geophysical Research* 109: C06026, DOI:10.1029/2003JC001823.

Shackleton NJ (1974) Attainment ofisotopic equilibrium between ocean water and the benthonic foraminifera genus *Uvigerina*: isotopic changes in the ocean during the last glacial. *Centre National de la Recherche Scientifique Colleagues Internationeau,* 219: 203-209.

Simstich J, Sarnthein M and Erlenkeuser H (2003) Paired delta O-18 signals of *Neogloboquadrina pachyderma* (s) and *Turborotalita quinqueloba* show thermal stratification structure in Nordic Seas. *Marine Micropaleontology* 48(1-2): 107-125.

Ślubowska M, Koç N, Rasmussen TL and Klitgaard-Kristensen D (2005) Changes in the flow of Atlantic water into the Arctic Ocean since the last deglaciation: Evidence from the northern Svalbard continental margin, 80^{o}N. *Paleoceanography* 20**:** PA001141, DOI:10.1029/2005PA001141

Spielhagen RF, Werner K, Sørensen SA et al. (2011) Enhanced Modern Heat Transfer to the Arctic by Warm Atlantic Water. *Science* 331: 450-453.

Stuiver M, Reimer PJ and Reimer RW (2005) CALIB 6.0. [WWW program and documentation].

Volkmann R (2000) Planktic foraminifers in the outer Laptev Sea and the Fram Strait - Modern distribution and ecology: *Journal of Foraminiferal Research* 30: 157-176.

Walczowski W, Piechura J, Osinski R and Wieczorek P (2005) The West Spitsbergen Current volume and heat transport from synoptic observations in summer. *Deep Sea Research Part I: Oceanographic Research Papers* 52: 1374-1391.

Walker M, Johnsen S, Rasmussen SO et al. (2009) Formal definition and dating of the GSSP (Global Stratotype Section and Point) for the base of the Holocene using the Greenland NGRIP ice core, and selected auxiliary records. *Journal of Quaternary Science* 24: 3-17.

Werner K, Spielhagen RF, Bauch D, et al. (2013) Atlantic Water advection versus sea-ice advances in the eastern Fram Strait during the last 9□ka – multiproxy evidence for a two-phase Holocene. *Paleoceanography*, 28(2), 283-295.

Wilson LJ, Hald M and Godtliebsen F (2011) Foraminiferal faunal evidence of twentieth-century Barents Sea warming. *The Holocene 21*(4): 527-537.

Zamelczyk K, Rasmussen TL, Husum K et al. (2012) Paleoceanographic changes and calcium carbonate dissolution in the central Fram Strait during the last 20 ka yr. *Quaternary Research* 78: 405-416.

Figure captions

Table 1. Radiocarbon dates and calibrations from core MSM5/5-712. The radiocarbon dates were performed by the Leibniz-Laboratory for Radiometric Dating and Isotope Research, Kiel, Germany (KIA) and at Poznań Radiocarbon Laboratory, Poland (Poz). A reservoir age correction of 400 years with an additional reservoir correction (ΔR) of 151±51 was used.

Figure 1. (A) Map of the north-eastern North Atlantic Ocean and adjoining seas showing the major currents systems and average position of the Polar and Arctic fronts modified from Marnela et al. (2008). Open circles indicate core location of Kastenlot core MSM05/5-712-2, giant box corer MSM05/5-712-1 and other cores mentioned in the text. Abbreviations: NAC: North Atlantic Current; IRM: Irminger Current; NwASC: Norwegian Atlantic Slope Current; NwAC: Norwegian Atlantic Current; WSC: West Spitsbergen Current; NCaC: North Cape Current; RAW: Re-circulating Atlantic Water; SB: Svalbard Branch; YSC: Yermark Slope Current; ESC: East Spitsbergen Current; EGC: East Greenland Current. (B) Conductivity, temperature, and depth (CTD). Eastern Fram Strait, August 2007.

Figure 2. Age model and sedimentation rate (cm/kyr) for Kastenlot core MSM05/5-712-2. Error bars show the 2σ standard deviation of the calibrated ages.

Figure 3. Correlation and regressions between Holocene Mg/Ca and other trace element rations in MSM05/5-712-2. Mg/Ca vs. (A) Al/Ca, (B) Mn/Ca and (C) Fe/Ca (contamination indicators).

Figure 4. Mg/Ca concentration and sediment TOC and $CaCO_3$ contents plotted against calibrated age and depth in core MSM05/5-712-2. (A, B) Sediment TOC and $CaCO_3$ contents (weight %) in core MSM05/5-712-2 (Grey: (Müller et al., 2012); Black: (Aagaard-Sørensen et al., submitted)). (C) Mg/Ca concentration (mmol/mol). Thin line = raw data. Thick line = 5-point running mean. Crosses mark omitted data points. Filled circle shows the average reproducibility of sample splits (±0.039 mmol/mol). (D) Reconstructed $sSST_{Mg/Ca}$. Present

day water temperatures at 50 and 200 m water depth are shown in grey fonts on Y-axis. Diamonds on X-axis indicate radiocarbon dated levels.

Figure 5. Reconstruction of $sSST_{Mg/Ca}$ compared to other marine proxies from core MSM5/5-712-2 and MSM5/5-712-1. (A) Ice-volume corrected *N. pachyderma* (sin) $\delta^{18}O$ record (grey line) with 3-point running mean (black line) from core MSM5/5-712-2 (Werner et al., 2013). (B) Reconstructed $sSST_{Mg/Ca}$ (black) (present study) shown with $sSST_{Mg/Ca}$ reconstruction from core MSM5/5-712-1 calculated using exponential temperature equation of Elderfield and Ganssen (2000) (Spielhagen et al., 2011) (purple) and linear temperature equation of Kozdon et al. (2009) (blue). Purple and blue dashed lines indicate calculated core-top $sSST_{Mg/Ca}$ (C) Reconstructed $sSST_{Mg/Ca}$ (black line) and $sSST_{Mg/Ca}$ based on Mg/Ca values that have been artificially increased 15 % (grey line). Summer sub sea surface temperatures (at 50 m water depth) calculated using the SIMMAX modern analogue technique from Spielhagen et al. (2011) (core MSM5/5-712-1) (purple) and Werner et al. (2013) (MSM5/5-712-2) (red) are also shown. Present day water temperatures at 50 and 200 m water depth are indicated on the y-axis to the right.

Figure 6. The reconstructed $sSST_{Mg/Ca}$ for the eastern Fram Strait compared with other proxy records and (sub)SST reconstructions in a south-north transect. (A) June insolation at 80°N (Berger and Loutre, 1991). (B) Sediment IP_{25} concentrations (Müller et al., 2012). (C) SiZer analysis of reconstructed $sSST_{Mg/Ca}$ from core MSM5/5-712-2. The SiZer map, a function of scale (y-axis: $\log_{10}(h)$) and location (x-axis: calendar age BP), shows at what given time the proxy record has significant increase (red), decrease (blue), no change (purple) or has insufficient observations for correct inference (grey). (D) Reconstructed $sSST_{Mg/Ca}$. Thin line = raw data. Thick line = 5-point running mean. (E) Transfer function summer sSST reconstructions at 50 m water depth (SIMMAX modern analogue technique) in core MSM5/5-712-2 (Werner et al., 2013). (F) Transfer function summer sSST reconstructions

662 100 m water depth (Weighted average partical least squares model) in core MD99-2304

663 (Ebbensen et al., 2007; Husum and Hald, 2012). (G) Transfer function based summer SST

664 reconstructions at 10 m water depth (Maximum Likelihood model) in Core 23258-2 (Hald et

665 al., 2007; Sarnthein et al., 2003). (H) Transfer function based summer SST reconstructions at

666 10 m water depth (Maximum Likelihood model) in Cores MD95-2011 and JM97-948/2A

667 (Hald et al., 2007; Risebrobakken et al., 2003).

668

Table 1

Core id	Lab. code	Depth range (cm)	Material	^{14}C age	Calibrated age ± 2σ	2 σ max cal. age (cal. age intercepts) 2 σ min cal. age	Reservoir age (R=400 + ΔR)	References
MSM5/5-712-2	KIA 45217	10-12	*N. pachyderma*	815±25	317±131	186(317)447	551±51	Werner et al., 2013
MSM5/5-712-2	KIA 41024	20-22	*N. pachyderma*	1570±25	972±141	831(972)1113	551±51	Werner et al., 2013
MSM5/5-712-2	KIA 45218	27-29	*N. pachyderma*	1985±25	1393±118	1275(1393)1510	551±51	Werner et al., 2013
MSM5/5-712-2	KIA 45219	40-42	*N. pachyderma*	2565±25	2056±165	1891(2056)2220	551±51	Werner et al., 2013
MSM5/5-712-2	SacA 19113	60-61	*N. pachyderma*	3365±30	3029±175	2854(3029)3203	551±51	Giraudeau (in prep)
MSM5/5-712-2	SacA 19114	94-95	*N. pachyderma*	4915±30	5041±189	4852(5041)5230	551±51	Giraudeau (in prep)
MSM5/5-712-2	SacA 19115	138.5-139.5	*N. pachyderma*	6440±30	6756±151	6605(6756)6906	551±51	Giraudeau (in prep)
MSM5/5-712-2	KIA 38080	168.5-169.5	*N. pachyderma*	7305 ±35	7630±126	7504(7630) 7756	551±51	Werner et al., 2013
MSM5/5-712-2	KIA 41025	191.5-192.5	*N. pachyderma*	7815±45	8133±157	7976 (8133) 8290	551±51	Werner et al., 2013
MSM5/5-712-2	Poz-30723	214-215	*N. pachyderma*	8362±45	8749 ±209	8540 (8749) 8958	551±51	Present study
MSM5/5-712-2	KIA 37423	280-281	*N. pachyderma*	9220±50	9797±252	9551 (9797) 10042	551±51	Present study
MSM5/5-712-2	Poz-30725	322-323	*N. pachyderma*	9580±47	10310 ±158	10152 (10310) 10468	551±51	Present study
MSM5/5-712-2	Poz-30726	428-431	*N. pachyderma*	12358±63	13629±197	13432 (13629) 13826	551±51	Present study

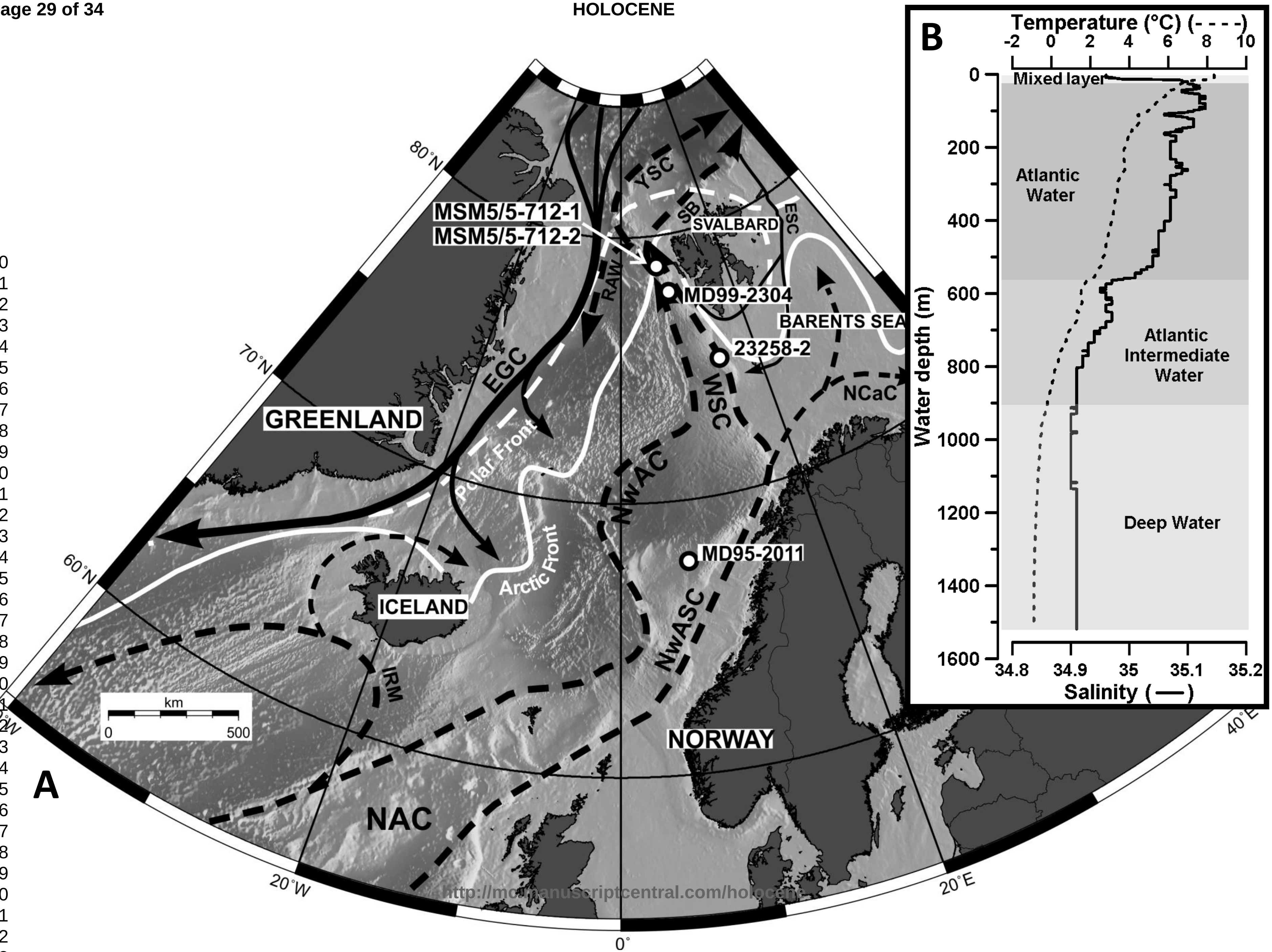
A
B
GREENLAND
ICELAND
NORWAY
SVALBARD
BARENTS SEA
MSM5/5-712-1
MSM5/5-712-2
MD99-2304
23258-2
MD95-2011
EGC
YSC
SB
ESC
RAW
WSC
NwAC
NwASC
NCaC
IRM
NAC
Polar Front
Arctic Front
80°N
70°N
60°N
40°W
20°W
0°
20°E
40°E
km
0
500
Temperature (°C) (- - - -)
-2 0 2 4 6 8 10
Mixed layer
Atlantic Water
Atlantic Intermediate Water
Deep Water
Water depth (m)
0 200 400 600 800 1000 1200 1400 1600
34.8 34.9 35 35.1 35.2
Salinity (—)

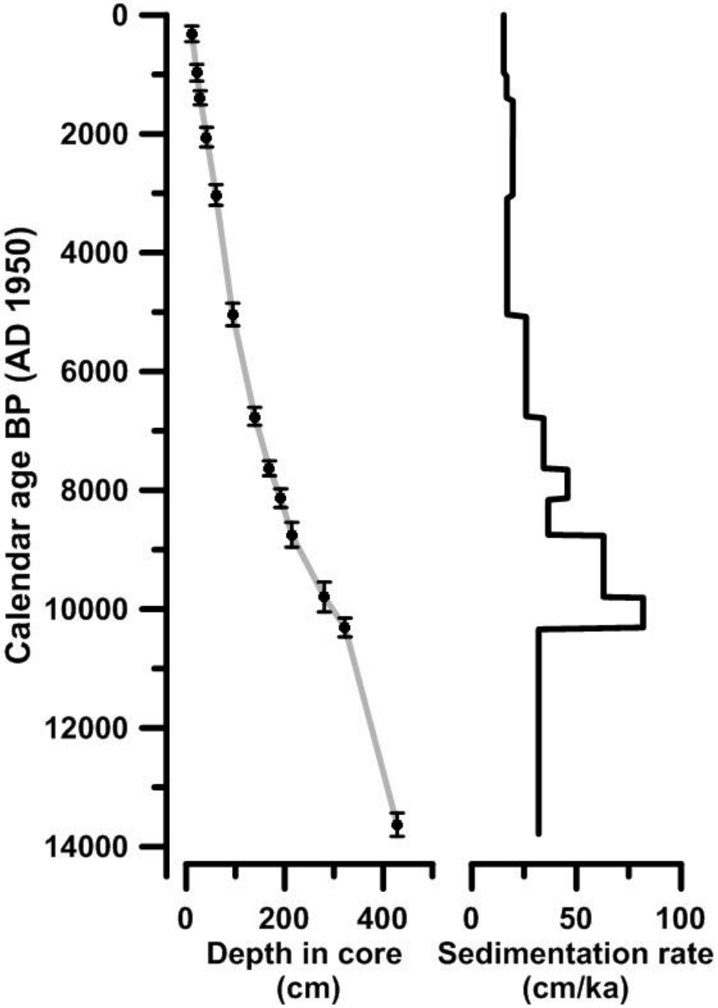
Calendar age BP (AD 1950)
0
2000
4000
6000
8000
10000
12000
14000
0
200
400
Depth in core
(cm)
0
50
100
Sedimentation rate
(cm/ka)

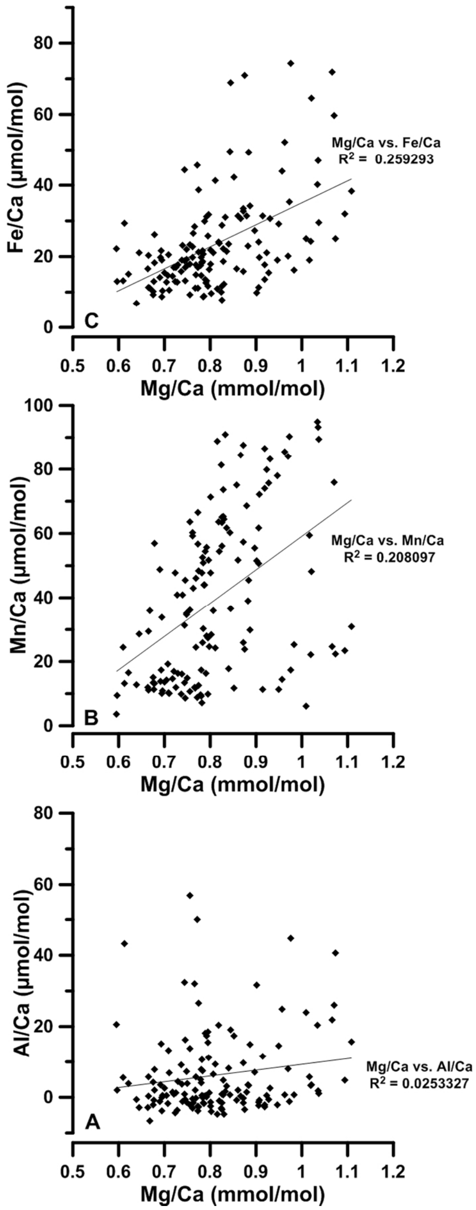

280x476mm (96 x 96 DPI)

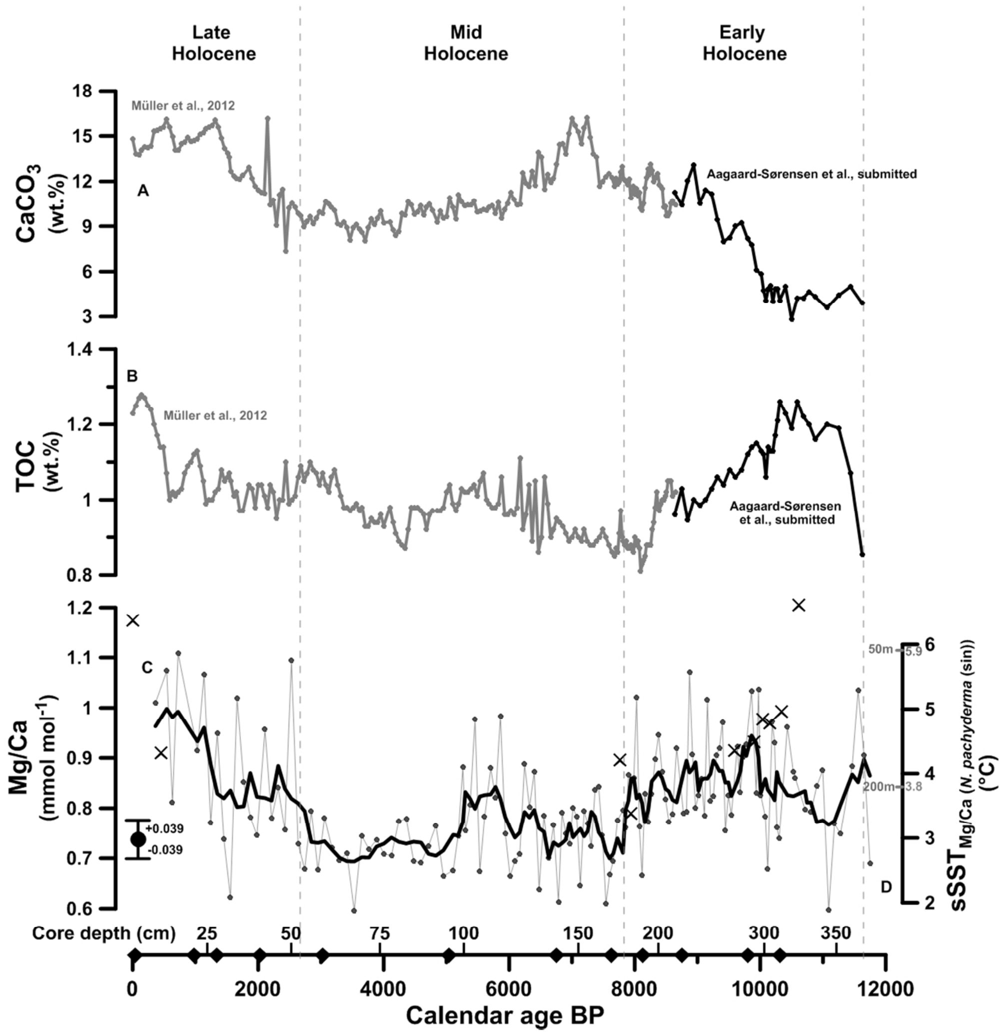

337x350mm (96 x 96 DPI)

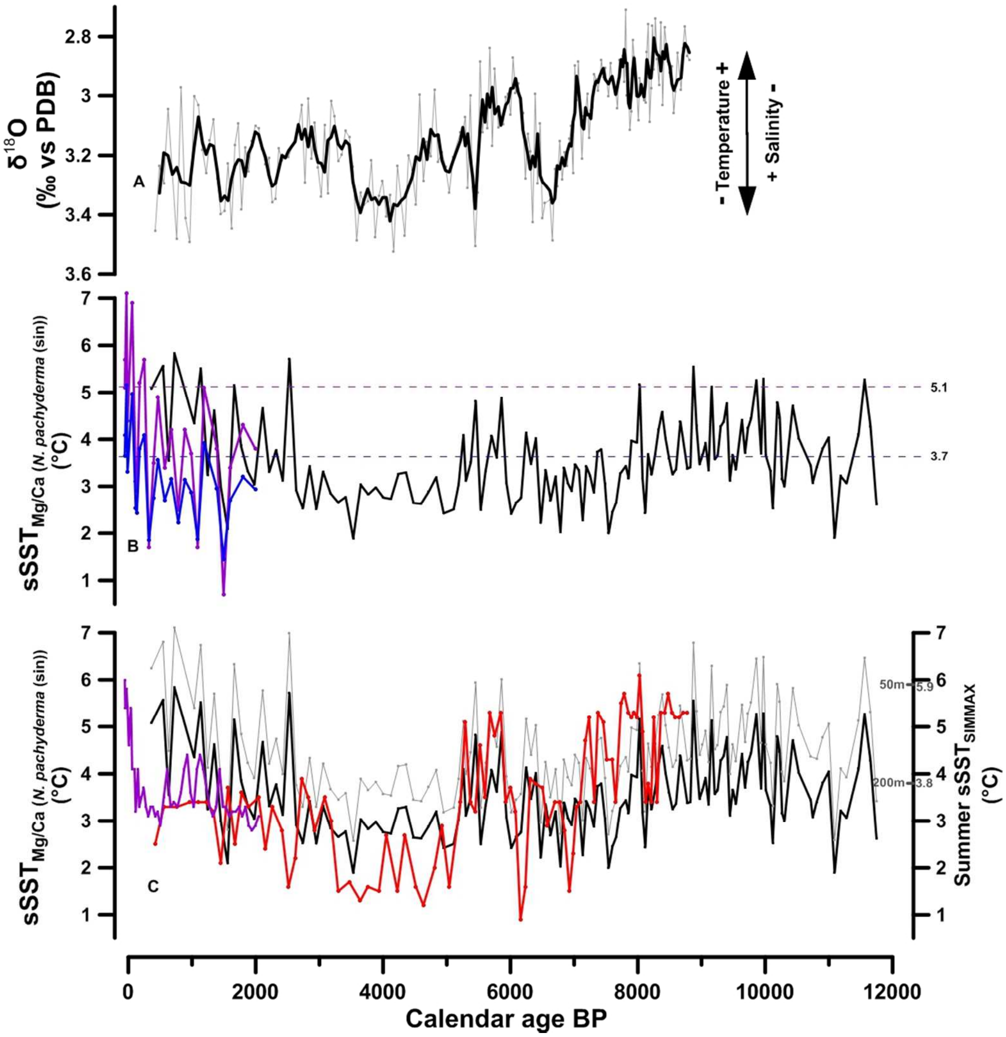

332x352mm (96 x 96 DPI)

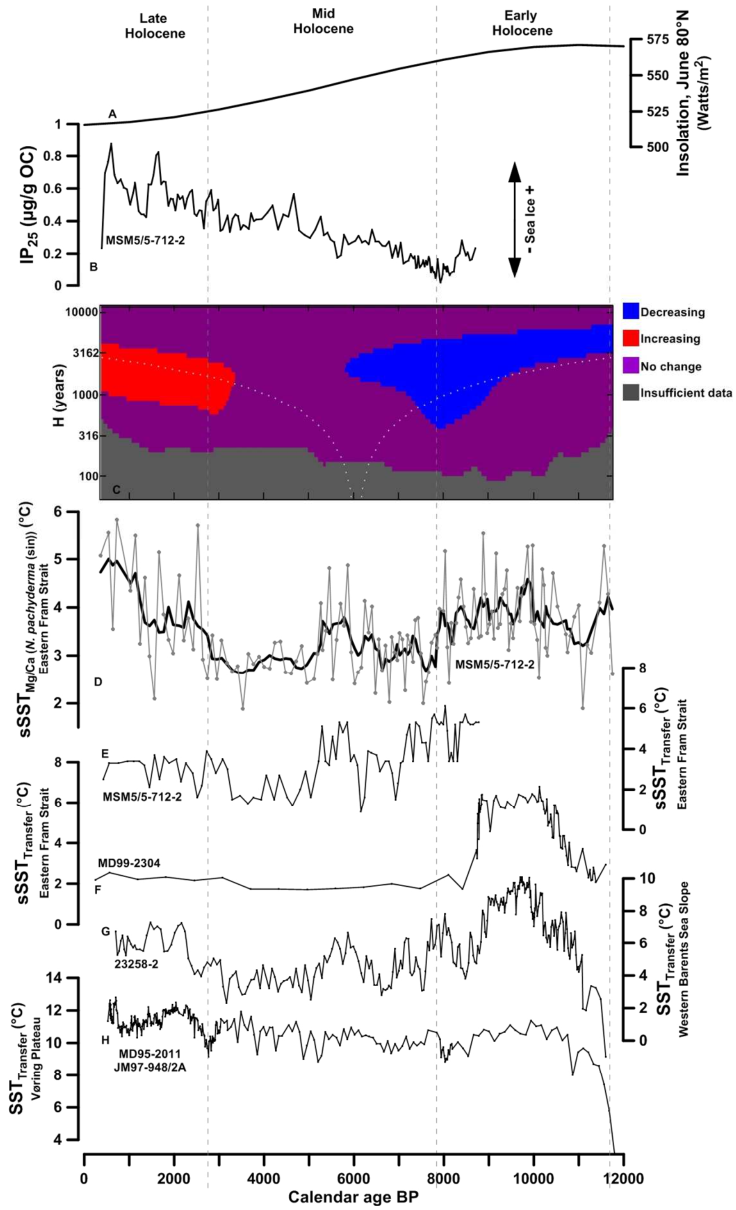

342x564mm (96 x 96 DPI)